Biogeochemistry (2011) 102:15–29
DOI 10.1007/s10533-010-9476-8

SYNTHESIS & EMERGING IDEAS

An open system framework for integrating critical zone structure and function

Craig Rasmussen · Peter A. Troch · Jon Chorover · Paul Brooks · Jon Pelletier · Travis E. Huxman

Received: 3 October 2008 / Accepted: 17 May 2010 / Published online: 15 June 2010

Abstract The "critical zone" includes the coupled earth surface systems of vegetation, regolith and groundwater that are essential to sustaining life on the planet. The function of this zone is the result of complex interactions among physical, chemical and biological processes and understanding these interactions remains a major challenge to earth system sciences. Here we develop an integrated framework based on thermodynamic theory to characterize the critical zone as a system open to energy and mass fluxes that are forced by radiant, geochemical, and elevational gradients. We derive a statement that demonstrates the relative importance of solar radiation, water, carbon, and physical/chemical denudation mass fluxes to the critical zone energy balance. Within this framework we use rates of effective energy and mass transfer [EEMT; W m^{-2}] to quantify the relevant flux-gradient relations. Synthesis of existing data demonstrates that variation in energetics associated with primary production and effective precipitation explains substantial variance in critical zone structure and function. Furthermore, we observe threshold behavior in systems that transition to primary production predominance of the energy flux term. The proposed framework provides a first order approximation of non-linearity in critical zone processes that may be coupled with physical and numerical models to constrain landscape evolution.

Keywords Critical zone · Open system thermodynamics · Energy and matter transfer · Pedogenesis · Biogeochemistry · Landscape evolution · Ecohydrology · Hydrologic partitioning

Electronic supplementary material The online version of this article (doi:10.1007/s10533-010-9476-8) contains supplementary material, which is available to authorized users.

C. Rasmussen (✉) · J. Chorover
Deparment of Soil, Water and Environmental Science, The University of Arizona, 1177 E. Fourth Street, Shantz Bldg., Rm. 429, Tucson, AZ 85721-0038, USA
e-mail: crasmuss@cals.arizona.edu

P. A. Troch · P. Brooks
Department of Hydrology and Water Resources, The University of Arizona, Tucson, AZ, USA

J. Pelletier
Department of Geosciences, The University of Arizona, Tucson, AZ, USA

T. E. Huxman
Department of Ecology and Evolutionary Biology, The University of Arizona, Tucson, AZ, USA

T. E. Huxman
B2 Earthscience, The University of Arizona, Tucson, AZ, USA

Introduction

What governs the structure and co-evolution of vegetation, soils, and landforms that comprise the Earth's critical zone? The "critical zone", defined as

the coupled earth surface systems of vegetation, regolith and groundwater (NRC 2001), acts as a living filter that controls the energy, water and carbon cycles, the fate and transport of nutrients and pollutants, and atmospheric composition, and hence is "critical" to supporting life on Earth (Chorover et al. 2007) (Fig. 1). The evolution and structural development of the critical zone is the result of complex interactions among physical, chemical and biological processes (Brantley et al. 2006). Understanding these interactions remains as a major challenge to the Earth sciences (NRC 2009; Sivapalan 2005). For example, soil horizons develop in response to radiant, geochemical and elevational gradients. These horizons, in turn, modify system hydrology and ecology in ways that Earth scientists have not been able to fully predict. Addressing the complexity of these interactions is central to improving our understanding of fundamental Earth surface processes such as terrestrial carbon cycling, mineral-microbe interactions, and the geologic and atmospheric controls of landscape evolution (NRC 2001). Here we address the need for a quantitative, cross-disciplinary and integrated framework that can help address this challenge using measured fluxes of energy and matter. Examples are provided to show associated predictions of critical zone structure and process.

The critical zone may be conceptualized as an integrated group of systems or structures that act to move energy and matter down gradients. Gradient driven energy and matter flux give rise to physical transport and chemical transformation that organize the critical zone, e.g., soil horizons, catenas, stream networks, vegetative structure, etc. Characterizing the movement and transformation of matter and energy within a system is a primary goal of thermodynamics. Thermodynamics are, therefore, a potentially powerful tool for integrating critical zone systems. The approach proposed here is an outgrowth of the work of Lotka (1922), Jenny (1941), Lindeman (1942) and Hutchinson (1957) on ecosystems and the initial development of ecosystem theory. These concepts have also been broadly applied across Earth science disciplines for modeling processes such as: the transfer of heat in the Earth's climate system (Kleidon and Lorenz 2005); the development of stream channel networks (Rinaldo et al. 1998); the complexity and organization of biological systems (Morowitz 1968; Odum 1988); and the rate and degree of soil formation (Blum 2008; Smeck et al. 1983; Volobuyev 1983). Here we integrate these concepts within an "open system thermodynamic" framework of gradient driven energy flow and mass transfer. The proposed framework quantifies interactions among critical zone systems using a common currency of "effective

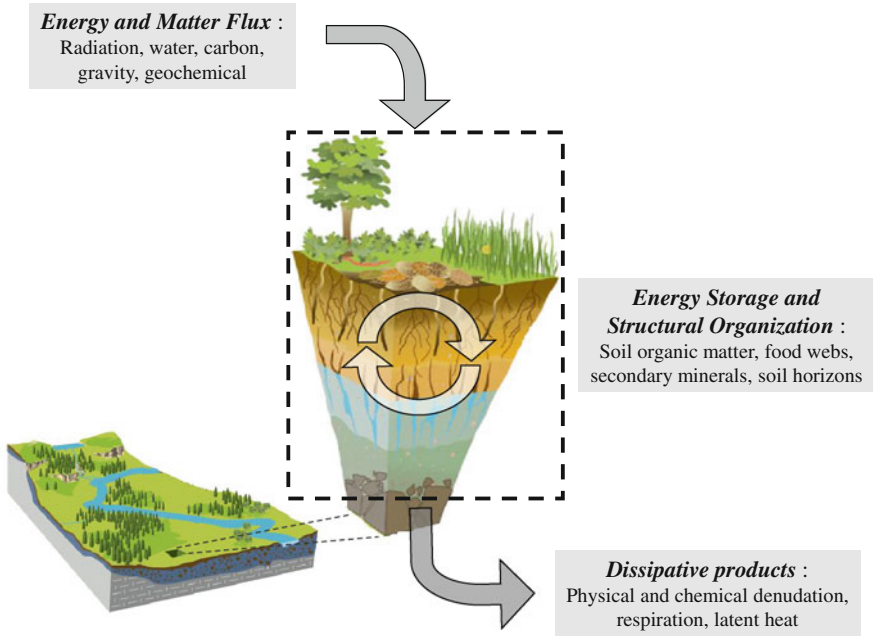

Fig. 1 Conceptual model of the critical zone system; the dashed line indicates the open system boundary as defined for the model derivation presented herein. The relative energy and mass transfer components include (i) energy and mass flux into the critical zone, (ii) energy storage within the critical zone, and (iii) export of dissipative products from the system to its surrounding environment. Figure modified from Chorover et al. (2007) and Rasmussen et al. (2005). Schema here is presented as vertical flow for simplicity of presentation, but the model is not limited to 1-dimensional fluxes

energy and mass transfer" (EEMT; units of [W m^{-2}]) that encompasses energy and matter transfer associated with primary production and regolith water flux (Rasmussen and Tabor 2007).

The objective of this paper is to synthesize theory that relates gradient driven energy and matter flux to critical zone structure and evolution. We begin with derivation of the open system construct, building from simple balance equations to open, non-equilibrium system thermodynamic principles. As a first-order test of the hypothesis, we use the framework to analyze a wide range of critical zone properties.

Theoretical construct

Energy and matter flux in critical zone systems

Characterization of any biophysical system first requires a clear definition of boundaries (Balzhiser et al. 1977). The critical zone extends from the top of the canopy (vegetation boundary layer) down to and including groundwater (Brantley et al. 2006). Here we focus on the upper portion of the critical zone, including vegetation and regolith (soil and saprolite), with the lower boundary at unweathered parent material (Fig. 1).

The flux of energy, water and carbon through the critical zone facilitates formation of critical zone "structures" that control the partitioning of energy and matter into storage, dissipative processes, and energetic transfers (Fig. 1). This partitioning is central to critical zone development and is the core of the theoretical construct developed below. The traditional framework of "soil forming factors" introduced by Dokuchaev (1967) and formalized by Jenny (1941) is our starting point for characterizing mass and energy flow. Jenny (1941) derived a quantitative statement of external factors driving critical zone development: $\Phi_{CZ} = f(cl, o, r, p, t)$, where Φ_{CZ} is either a specific property of the critical zone, e.g., vegetation structure or soil clay content, or a set of properties that describe critical zone state at a given time; and climate (cl), organisms (o), relief (r), parent material (p), and age of system (t) are constraining factors. Jenny (1961) revised this equation into the general form:$\Phi_{CZ} = f(P_x, L_o, t)$, where P_x encompasses external energy and mass fluxes including solar radiation (E_{SOLAR}), precipitation (P), and carbon from primary production (C) [i.e., $P_x = f(E_{SOLAR}, P, C)$], and L_o is initial state of the system, including relief and parent rock type.

Building upon this and other work relating energy potentials to pedogenesis (Runge 1973; Smeck et al. 1983), Rasmussen et al. (2005) and Rasmussen and Tabor (2007) quantified P_x to the subsurface in terms of effective energy and mass transfer (EEMT). EEMT includes inputs of energy associated with reduced carbon from primary production [E_{BIO}] (Lieth 1975) and heat influx to soil from precipitation minus evapotranspiration and surface runoff [E_{PPT}] (Arkley 1963):

$$\text{EEMT} = E_{BIO} + E_{PPT} \quad \left[\text{W m}^{-2}\right] \tag{1}$$

Rasmussen and Tabor (2007) demonstrated strong, significant relations between EEMT and quantifiable soil properties for free-draining, minimally-erosive landscapes across a range of environmental gradients. The same soil variables showed weak relation to annual temperature or precipitation, indicating EEMT was more effective at describing the energy fluxes driving soil development than temperature or precipitation alone.

Employing the generalized form of Jenny's equation in the new form: $\Phi_{CZ} = f(\text{EEMT}, L_o, t)$, one can predict critical zone structure in an open system thermodynamic context. Here we expand on this framework, introducing additional energy and mass flux terms, and use simple energy and mass balance to demonstrate how open system thermodynamic theory may be quantitatively applied to the critical zone system.

Component balance equations

The key energetic potentials and fluxes that drive critical zone formation may be summarized as (i) radiant energy flux from solar radiation, (ii) water mass balance, (iii) carbon mass balance, and (iv) landscape physical and chemical denudation. Below, we outline simple balance equations for each component and place them in the context of an overall critical zone energy balance.

Radiant energy balance

Solar radiation is by the far the dominant energy source to critical zone systems (Table 1). Net radiant energy

Table 1 Maximum values for critical zone energy input and fluxes

Flux component	Maximum flux MJ m^{-2} yr^{-1}
Solar absorption, terrestrial[a]	5.7×10^6
E_{ET} (latent heat flux from terrestrial evapotranspiration)[a]	3.7×10^5
E_{PPT} (energy flux from effective precipitation)[b]	650
E_{BIO} (energy flux from net primary production)[b]	57
E_{ELV} (energy flux from uplift and/or physical denudation)[a]	1.1
E_{GEO} (energy flux from chemical denudation)[c]	0.7
ξ (energy flux from anthropogenic and/or dust)[d]	0.08–0.2

All of the fluxes are inputs except for terrestrial latent heat flux that is lost from the critical zone to the atmosphere

[a] Data taken from Phillips (2009) and references therein

[b] Data based on global climate dataset of New et al. (1999) and calculated according to Rasmussen et al. (2005)

[c] Maximum chemical denudation energy estimated from maximum rate of watershed Na efflux (White and Blum 1995) and Gibb's energy of reaction assuming complete dissolution of albite and 262 kJ/mol Na

[d] Anthropogenic data estimated assuming NH_4SO_4 fertilizer application at a rate of 200 lbs/acre and a chemical potenital of NH_4SO_4 of 901 kJ/mol. The dust energy flux calculated assuming maximum dust input of 20 g/m^2/yr (Reheis 2006) and that all dust is in the form of the mineral muscovite with a chemical potential of 5558 kJ/mol (Woods and Garrels 1987)

(R_N) to the critical zone is the additive result of latent heat dissipated via evapotranspiration (λET), the fraction of photosynthetically active radiation partitioned to biomass production during photosynthesis (λBIO), net sensible or long-wave radiative heat flux (H), and heat flux into the ground (G) (Evett 2000):

$$R_N = \lambda ET + \lambda BIO + H + G \quad \left[J\ m^{-2}\ s^{-1}\right] \qquad (2)$$

Since most radiant energy is returned back to the atmosphere via ET and H, and the net ground flux is generally at or near zero over annual time scales, the most substantial radiant flux into the subsurface critical zone is associated with λBIO, i.e., energy used for primary production that results in energy stored as fixed carbon in biomass and humus. Most hydrologic and soil physical models do not include the λBIO term because it represents a minor fraction of the net energy balance, i.e., <1% of total incoming solar radiation (Botkin and Malone 1968; Reiners 1972).

Water mass balance

The net water balance can be described in terms of soil or watershed wetting using a catchment scale approach that is also applicable at the pedon scale (water mass flux derived from precipitation depth and assuming water density of 1.0 kg dm^{-3}) (L'vovich 1979):

$$W = P - SR = ET + F + BIO \quad \left[kg\,m^{-2}s^{-1}\right] \qquad (3)$$

where W is subsurface or watershed wetting, P is precipitation, SR is quick surface runoff, ET is mass of water returned to the atmosphere via evapotranspiration, F is mass flux to base flow and equivalent to the fraction of precipitation available to flux through and out of the soil, and BIO is mass of water partitioned to primary production. The F term exerts strong control over the rate and trajectory of geochemical weathering, including associated solute and colloid flux. Similar to the energy balance, the BIO term is generally not considered significant in terms of catchment water balance; it is small relative to evapotranspiration and base flow, on the order of 0.1% of the relative water mass partitioned to transpiration (see below).

Carbon mass balance

The net flux of carbon through the critical zone, or "net ecosystem exchange" (NEE), incorporates production, loss and transformation (Lovett et al. 2006): $NEE = GPP - Ox + CE^*$ [kg m^{-2} s^{-1}], where gross primary production (GPP) is balanced by oxidative losses (Ox) such as autotrophic and heterotrophic

respiration, and abiotic losses to fire or ultraviolet oxidation, plus the net balance of solid- or solution-state carbon inputs and exports (CE*) such as carbon flux associated with sediment transport, or solution-state fluxes of dissolved organic and inorganic carbon.

Gross primary production is the dominant carbon flux into the critical zone and includes the total CO_2 and H_2O transformed into fixed organic compounds and oxygen via photosynthesis: $6CO_2 + 6H_2O \xrightarrow[\lambda BIO]{} C_6H_{12}O_6 + 6O_2$, with CO_2 derived from the atmosphere, H_2O sourced from the subsurface critical zone and equivalent to the BIO fraction of the water balance, and λBIO is the fraction of incoming short-wave solar radiation used to drive the reaction forward. Photosynthesis is accompanied by substantial water loss to the atmosphere via transpiration. Gross primary production is thus a central process linking radiant energy and water balances through fixation of carbon and water into reduced organic compounds and latent heat flux associated with transpiration. Given that 1 mol of water is converted to biomass per mol CO_2 fixed, the partitioning of water to fixation (BIO) and transpiration (Tr) via photosynthesis may be quantified as water use efficiency (WUE) (Schlesinger 1997): WUE = BIO/Tr [mol mol^{-1}], with typical water use efficiencies ranging from 0.00085 to 0.0015 (Osmond et al. 1982). The small fraction of water partitioned to BIO highlights its exclusion from typical water balance statements as noted above. However, the flux of reduced carbon into the critical zone is central to powering biological systems, such that even the small fraction incoming radiation and water partitioned to primary production (ignored in most radiant and water balance statements) drives many critical zone processes.

A substantial fraction, on the order of 50% (Farrar 1985), of GPP is transformed back to CO_2 and water and transferred to the atmosphere or into the subsurface as a result of plant metabolic processes, i.e., plant respiration (PR). The net transfer of primary production into the critical zone as reduced organic carbon is thus equivalent to net primary production (NPP):

$$\mathrm{NPP} = \mathrm{GPP} - \mathrm{PR} \quad \left[\mathrm{kg\ m^{-2} s^{-1}}\right] \tag{4}$$

A limitation of using NPP to quantify carbon mass flux into the critical zone is that by definition, it does not include the mass fraction of GPP transferred to the subsurface as CO_2 from plant respiration that actively participates in mineral weathering (carbonation) reactions. Despite this limitation, we focus on NPP for the model derivation below because of the importance of reduced organic matter input as an energy source to soil food webs (Odum 1988) and soil formation (Buol et al. 2003), and the difficulty in partitioning plant respiration to above and below ground fluxes.

Physical and chemical denudation mass balance

The dominant external factors controlling landscape denudation include uplift rate and geochemical potential. These factors interact with radiant energy, water and carbon fluxes via regolith production, sediment transport and chemical weathering in a complex manner. Recent advances attempting to quantify these complex interactions have partitioned total denudation to physical and chemical mass flux terms that at steady-state is equivalent to (Riebe et al. 2001):

$$U = \mathrm{TD} = \mathrm{PD} + \mathrm{CD} \quad \left[\mathrm{kg\,m^{-2} s^{-1}}\right] \tag{5}$$

where U is the product of uplift rate [m s^{-1}] and rock density [kg m^{-3}], total denudation (TD) is the total mass lost, or denuded, from a landscape that is partitioned into mass loss associated with physical denudation (PD, i.e., sediment transport), and chemical denudation (CD, i.e., solute transport). Denudation ultimately represents a balance of uplift and soil/sediment production where the soil production rate characterizes either the conversion rate of bedrock to regolith on hillslopes via physical and chemical processes, or the wear/incision rate of rock by concentrated flow in channels (Dietrich et al. 2003). The potential for physical denudation is driven largely by local elevation gradients and the potential energy associated with sediment stored at a given elevation (Phillips 2009). The rate of physical denudation is locally controlled by the interaction of this potential with topography, regolith thickness and factors such as vegetation cover and soil organic matter content that control hillslope diffusivity (Pelletier 2008).

Chemical denudation includes the loss of soluble weathering products resulting from mineral dissolution. It is controlled by the geochemical potential of regolith and parent material, the interaction of that

potential with uplift and rate of mineral supply, and the through flux of water and carbon. This interaction may be demonstrated using a simple chemical reaction describing the hydrolytic and incongruent transformation of albite to kaolinite: $2NaAlSi_3O_8 + 9H_2O + 2H_2CO_3 \rightarrow Al_2Si_2O_5(OH)_4 + 2Na^+ + 2HCO_3^- + 4H_4SiO_4$, where the reactants include lithogenic albite, the supply of which is controlled by uplift and soil production, water in excess of surface runoff and ET (i.e., F in Eq. 3), and CO_2 from the atmosphere that is augmented by heterotrophic and autotrophic respiration and takes the form of carbonic acid when dissolved in water. Products include the secondary phase kaolinite and soluble products that may be leached away from the reaction zone with hydrologic flow. Quantitative methods for determining chemical denudation include those developed for solid and solution state fluxes over both long and short temporal scales (e.g., Riebe et al. 2001; White and Blum 1995).

Coupled critical zone energy and mass balance

Conversion of mass flux to energetic terms

Critical zone formation is the result of superimposed fluxes of radiant energy, water, carbon, and denudation (Phillips 2009; Smil 1991; Volobuyev 1974). Common dimensionality is required to evaluate their additive effects. Inclusion of radiant energy components suggests the utility of energy flux terms [J m^{-2} s^{-1} or, equivalently, W m^{-2}], which necessitates conversion of mass fluxes to the same units (made possible by the fact that 1 J = 1 kg m^2 s^{-2}). These conversions are outlined below.

The energy and mass flux associated with evapotranspiration, E_{ET}, may be stated: $E_{ET} = ET \cdot h_v$ [W m^{-2}], where ET is mass flux of precipitation to evapotranspiration [kg m^{-2} s^{-1}], and h_v is latent heat of vaporization [J kg^{-1}] and quantifies the fraction of radiant energy used to evaporate a mass of water. As noted above, this energetic flux is largely fluxed out of the critical zone and returned back to the atmosphere.

Water mass flux (F) can be converted to energy flux, denoted as E_{PPT}: $E_{PPT} = F \cdot c_w \cdot \Delta T$ [W m^{-2}], where F is mass flux of precipitation to base flow from the water balance [kg m^{-2} s^{-1}], c_w is specific heat of water [J kg^{-1} K^{-1}], and $\Delta T = T_{ambient} - T_{ref}$ where $T_{ambient}$ is taken as the ambient water temperature at the time of water flux and T_{ref} is a reference temperature. Here and in previous applications of the EEMT model, $T_{ambient}$ was assumed equal to the ambient air temperature, and T_{ref} was set to 273 K with the assumption that frozen water performs little work in terms of chemical and biological processes or mass flux through the soil (for times where $T_{ref} > T_{ambient}$, E_{PPT} is set equal to zero). We recognize work done by freeze–thaw and that chemical/biological processes occur at low temperatures, but in the current formulation these are not considered.

Carbon mass flux (NPP) can be converted to energy flux, denoted as E_{BIO}, where $E_{BIO} = NPP \cdot h_{BIO}$ [W m^{-2}], NPP is net primary production [kg m^{-2} s^{-1}], and h_{BIO} is the specific biomass enthalpy [J kg^{-1}]. We assume an average h_{BIO} of 22×10^6 J kg^{-1} biomass based on the average of values for a range of organic materials derived from calorimetric analyses (Leith 1975).

Physical denudation may be expressed in energy flux units as E_{ELV}, based on the change in potential energy of uplifted sediment (Phillips 2009): $E_{ELV} = m \cdot g \cdot U$ [W m^{-2}], where m is mass of sediment per unit area [kg m^{-2}], g is the gravitational constant [9.81 m s^{-2}], and U is uplift rate [m s^{-1}]. The mass of sediment available for transport may be approximated using rock density, ρ [kg m^{-3}] and regolith depth, H_S [m], where $m = \rho \cdot H_S$, assuming all soil and saprolite layers have the potential to be physically transported.

The mass and energy flux associated with chemical denudation and specific mineral transformations, E_{GEO}, may be approximated using the Gibbs energy (ΔG_R, J mol^{-1}) of a given mineral transformation reaction (determined for the relevant environmental conditions) and the associated mass flux (Bejan 2006): $E_{GEO} = N\Delta G_R$ [W m^{-2}], where N, the mass flux per unit area [mol m^{-2} s^{-1}], is a function of reaction rate and a stoichiometric coefficient (White and Brantley 2003).

Critical zone energy balance

The balance of energy and mass flux involved in critical zone development (Λ) may then be stated as (Volobuyev 1964):

$$\Lambda = E_{ET} + E_{PPT} + E_{BIO} + E_{ELV} + E_{GEO} + \xi \quad \left[\mathrm{W\,m^{-2}}\right] \tag{6}$$

where the first five terms are as defined above and ξ encompasses net energy flux associated with any additional material flux into the system such as dust, atmospheric solutes, or anthropogenic inputs such as fertilizers or other amendments. In general, these additional energetic fluxes are negligible relative to the other terms (Table 1), but may be relevant for specific ecosystems. The relative magnitude of the individual fluxes over annual time scales indicate latent heat transfer by evapotranspiration is the largest energy flux; however, as noted above this energy is largely transferred out of the critical zone back to the atmosphere and hence has a less direct impact on subsurface development (Table 1). Given the range of values, the key parameters for quantifying the flux of energy into and through the subsurface critical zone are E_{PPT} and E_{BIO}. These parameters describe the fraction of energy and mass effectively transferred into and through the subsurface critical zone and are the two parameters originally included in the EEMT term [see Eq. 1].

The critical zone as an open thermodynamic system

Exergy storage, flow and destruction

When superimposed on the systems-based approach of Jenny (1941), the energy balance outlined above provides a departure point for a thermodynamic approach to critical zone development (see *Supplemental Documents* for full thermodynamic derivation and referencing). Briefly, the First Law of Thermodynamics states that the change in state or internal energy storage of a system is equivalent to the energy flux through the system minus any work performed within or outside of the system. The critical zone energy balance, Λ, is thus equivalent to energy flux through the system, and equivalent to the amount of work the system can perform. Also central to thermodynamics is the concept of the irreversible conversion of available work energy to a form that is incapable of performing work, i.e., entropy production, as described in the Second Law.

The First and Second Law concepts have been coupled and applied to ecological systems using the engineering based concept of "exergy" (χ), which is a measure of the change in free energy for a system that can exchange pressure–volume work with its external environment (Bendoricchio and Jorgensen 1997; Kay 2000; Wagendorp et al. 2006):

$$\Delta\chi_{STORED} = \chi_{FLOW} - \chi_{DESTROYED} \quad \left[\mathrm{W\,m^{-2}}\right] \tag{7}$$

where $\Delta\chi_{STORED}$ is change in exergy stored in the system or "non-flow" exergy, χ_{FLOW} is flux of exergy through the system or Λ, and $\chi_{DESTROYED}$ is exergy destruction or the irreversible conversion of available work energy to entropy. For non-equilibrium systems exergy destruction is equivalent to $T\sigma$ where T is system temperature [K], and σ is the local rate of internal entropy production [W m^{-2} K^{-1}]. Assuming the change in critical zone state is equivalent to change in exergy storage, the system exergy balance may be restated for the critical zone as: $\Delta\Phi_{CZ} = \Lambda - T\sigma$ [W m^{-2}], and the generalized statement of Jenny reformulated as: $\Phi_{CZ} = f(\Lambda, T\sigma, t)$ [J m^{-2}], where the critical zone state (quantified as energy stored per unit area) is a function of exergy flow rate, local entropy production rate, and time. As noted above, the dominant components of Λ that flux into the critical zone are E_{PPT} and E_{BIO}, indicating these parameters may be used as a first order measure of flow exergy for predicting critical zone development.

Based on thermodynamic theory, it is posited that quantifying system flow exergy provides a direct measure of the function and structural/temporal organization of that system, as well as a means to identify energetic thresholds and transitions to nonlinearity in critical zone properties. Briefly, systems respond to flow exergy with the formation of structures that maximize exergy throughflow and degrade the flow exergy as quickly and efficiently as possible, thus evolving the system to a "far-from-equilibrium" steady-state where $\chi_{FLOW} = \chi_{DESTROYED}$, and $\chi_{STORED} > 0$ (Dewulf et al. 2008; Kay 2000). The internal structures resulting from this process require flow exergy to maintain them (Morowitz 1968) and the system partitions flow exergy to non-flow exergy (i.e., storage) at rates proportional to exergy flow rates (Jørgensen and Fath 2004). Increased storage of non-flow exergy pushes the system towards far-from-equilibrium conditions where multiple steady-state

configurations become possible (Nicolis and Prigogine 1989). In response to the departure from equilibrium, systems transition non-linearly to the configuration that yields both the greatest non-flow exergy storage and the greatest exergy throughflow, i.e., the configuration with the most ordered structure and largest gradients (Jorgensen and Fath 2006; Odum and Pinkerton 1955). The corollary of this concept is that of "maximum entropy production", which postulates that systems develop internal structures that simultaneously maximize the rate of internal entropy production and the rate of entropy export to the surrounding environment in response to gradients and exergy flux (Kleidon 2009). The development of these structures corresponds to spatial and temporal organization and hence *entropy minimization within the system*.

The optimization of system exergy flux, storage and destruction has thus been used as a goal function for ecosystem development in ecological modeling (e.g., (Bastianoni et al. 2006). For example, primary production may be considered an ecosystem structure that degrades the radiant energy flux from solar radiation and precipitation (flow exergy) through the process of evapotranspiration (exergy destruction). Primary production produces energy-rich material that is stored in living biomass and regolith as organic matter (non-flow exergy). Energy-rich organic matter is then used to facilitate further primary production through decomposition and nutrient supply such that storage and decomposition rates are optimized to maintain maximum productivity (Anderson 1995). Specifically, energy-rich organic matter serves as the main energy source powering soil food webs that result in organic matter decomposition and further exergy degradation via regolith volumetric expansion, mineral dissolution, and soil production, all of which serve to optimize primary productivity and degrade the radiant gradient.

The above derivation suggests open system thermodynamic theory provides a useful theoretical framework for (i) quantifying the potential energy stored within the critical zone, (ii) measuring critical zone structural organization; and (iii) identifying thresholds where non-linearities in critical zone organization and function occur. Given the dominance of critical zone flow exergy by EEMT, we hypothesize that: *EEMT drives regolith evolution, water residence time and biogeochemistry and thus provides a measure for predicting CZ structure and function*.

Synthesis of energy model application to critical zone systems

We present a synthesis of data spanning natural geochemical and radiant gradients under the context of the thermodynamic framework presented above, and relate effective energy and mass transfer to measures of critical zone structure and function. This synthesis provides a first order test of the hypothesis that EEMT exerts a primary control on critical zone development. Detailed discussion of datasets and data analyses is presented in the *Supplemental Documents*.

Global patterns of effective energy and mass transfer

Global scale EEMT patterns indicate clear variation in both the total flow exergy, EEMT, and the relative partitioning of exergy to primary production, E_{BIO}, and heat flux, E_{PPT}, components by latitude and ecosystem (Fig. 2 and Table 2). Briefly, high latitude sites are typified by relatively low flow exergy (i.e., EEMT less than 10 MJ m^{-2} yr^{-1} at latitudes greater than 65°), with a general increase in both EEMT amount and variance towards the equator (Fig. 2a). Tropical latitude EEMT values encompass the range of the entire dataset resulting from local variation in radiation and precipitation gradients; values range from near zero to over 290 MJ m^{-2} yr^{-1}. The global EEMT data further indicate a transition in the relative dominance of exergy partitioning to carbon and water near an EEMT value of 70 MJ m^{-2} yr^{-1} (Fig. 2b). This point corresponds to the transition from subtropical to tropical latitudes (Fig. 2a), the shift from subtropical and tropical grasslands to moist tropical forests (Table 2), and marks the transition to maximum ecosystem NPP (Table 2). This break point has substantial implications for critical zone function and development and may represent a critical threshold or point of nonlinearity in critical zone processes that will be explored further below.

The EEMT data may thus be grouped into two sets using the 70 MJ m^{-2} yr^{-1} break point identified in Fig. 2b: (i) "low" EEMT dominated by E_{BIO}; and (ii) "high" EEMT dominated by E_{PPT}. Low EEMT dominated by E_{BIO} represents "water-limited" systems where the majority of precipitation inputs are partitioned to a combination of surface runoff, ET and primary production, with little water available to

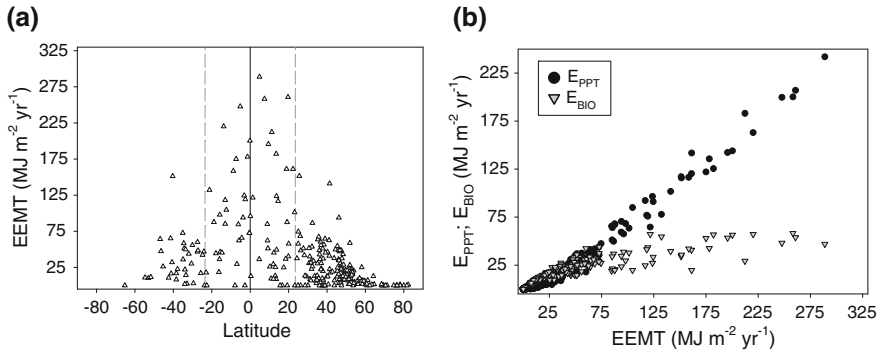

Fig. 2 Global distribution of **a** effective energy and mass transfer (EEMT) by latitude and **b** the relative fraction of EEMT derived from net primary production (E_{BIO}) and effective precipitation (E_{PPT}) with increasing EEMT. Data were derived from the IAEA ISOHIS dataset (http://www-naweb.iaea.org/napc/ih/IHS_resources_ISOHIS2.html) with EEMT calculated on a monthly time scale following Rasmussen et al. (2005). The equator and tropical latitudes are noted in **a** with the solid black line and the dashed gray lines, respectively

Table 2 Median climatic, latitude, and EEMT values derived from the IAEA ISOHIS[a] dataset for terrestrial ecoregions accroding to the WWF[b] dataset

Biome	*n*	Latitude Absolute degree	MAT °C	MAP mm	NPP g m^{-2} yr^{-1}	EEMT MJ m^{-2} yr^{-1}	F_{BIO} %
Tropical and subtropical forests	30	16	25	1,512	1,202	74	38
Tropical and subtropical grasslands, savannas, and shrublands	15	16	23	1,015	911	46	43
Temperate coniferous forests	14	47	9	996	711	28	64
Temperate broadleaf and mixed forests	14	49	10	761	673	27	57
Mediterranean scrub	51	37	16	550	539	12	76
Temperate grasslands, savannas, and shrublands	15	41	10	550	430	11	81
Boreal forest/taigas	13	60	0	474	89	2	88

[a] ISOHIS climate dataset available at http://www-naweb.iaea.org/napc/ih/IHS_resources_ISOHIS2.html

[b] WWF terrestrial ecoregion dataset available at http://www.worldwildlife.org/science/data/terreco.cfm

Sample number *n* notes the number of ISOHIS weather stations in a specific biome. Only biomes with >10 stations are reported

flux through the critical zone. Furthermore, dominance by E_{BIO} indicates that the dominant form of flow exergy through the system is in the form of organic carbon, such that carbon cycling likely dominates the exergy storage and exergy destroying structures formed within the system. In contrast, high EEMT systems dominated by E_{PPT} represent "energy-limited" systems with abundant precipitation in excess of runoff, ET and primary production, and thus the potential for substantial water flux through the critical zone. The dominant form of flow exergy in these systems is thus heat flux associated with water moving through the subsurface critical zone and suggests evolution of a different set and/or additional exergy storage and destruction structures relative to low EEMT sites; structures such as those associated with mineral transformation and chemical denudation, e.g., deep, chemically depleted regolith.

Given the potential significance to critical zone structural evolution of this transition, we define a dimensionless term, F_{BIO}, that quantifies the relative partitioning of EEMT to primary production: $F_{BIO} = E_{BIO}/EEMT$. The remaining analyses will focus on comparative analysis of critical zone properties to both the magnitude of EEMT and F_{BIO} with the intent of identifying changes and nonlinearity in critical zone processes with increasing EEMT and carbon to water partitioning.

Effective energy and mass transfer and landscape denudation

Physical and chemical denudation result from complex interactions among uplift rate and landscape geochemical potential with energy, water and carbon fluxes. Here we compare short-term watershed-based chemical denudation rate data, and long-term regolith-based physical and chemical denudation rates with EEMT and F_{BIO}. The current analyses focus on critical zone systems formed in granitic terrain to provide constraint over variation in landscape geochemical potential. This constraint allows for more direct comparison of denudation data to energy and mass flux terms across a wide range of sites without having to account for large lithologic differences.

Measures of chemical denudation at the watershed scale in the form of Si-efflux in surface waters (White and Blum 1995; White et al. 1999) demonstrate significant linear relationships with EEMT (Fig. 3). In particular, watersheds in which EEMT is dominated by E_{PPT}, i.e., $F_{BIO} < 0.5$, the Si-efflux is highly and linearly correlated with EEMT ($R^2 = 0.80$; $P < 0.001$), whereas EEMT exhibits weaker relation to Si-efflux for low EEMT sites with $F_{BIO} > 0.5$. The clear break in the relation of chemical denudation to EEMT at F_{BIO} of 0.5 indicates varying critical zone response to flow exergy relative to the partitioning of that exergy to carbon and water. As noted above, E_{BIO} dominated low EEMT sites have little water available to flux through the critical zone, thus limiting chemical weathering reactions and solute export. In contrast, the strong linear relation in E_{PPT} dominated high EEMT sites indicates tight coupling of chemical denudation to exergy flux from water and heat transfer through the critical zone.

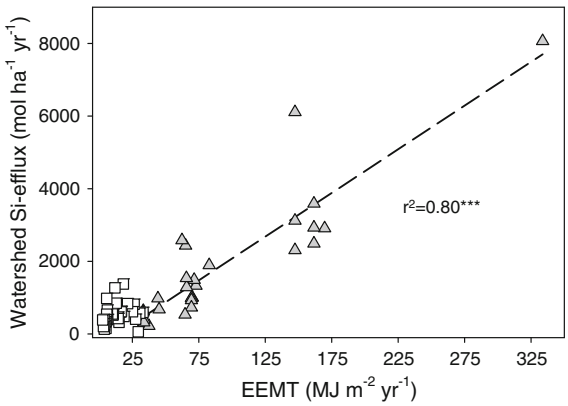

Fig. 3 Watershed Si-efflux in surface water, a proxy for chemical denudation rate, relative to EEMT. The open squares are sites where the fraction of EEMT from net primary production (F_{BIO}) is less than 0.5 whereas gray triangles are sites of $F_{BIO} < 0.5$. The dashed line is the regression line between EEMT and Si-efflux for sites with $F_{BIO} < 0.5$. Watershed data from White et al. (1999) and White and Blum (1995) and EEMT calculated from mean annual temperature and precipitation following Rasmussen and Tabor (2007)

Regolith based measures of physical and chemical denudation (Riebe et al. 2004) are linearly related to EEMT for sites dominated by E_{PPT}, but not for sites dominated by E_{BIO} (Fig. 4a, c). The chemical depletion fraction, i.e., the fraction of total denudation attributable to chemical denudation, also demonstrates a threshold-like function with increasing EEMT at the F_{BIO} equal to 0.5 transition (Fig. 4b). The combined data suggest a clear shift in critical zone structure and function at the transition from carbon to water dominated exergy flow. The linear trends for high EEMT sites indicate decreasing denudation rates and a greater fraction of denudation partitioned to chemical weathering with increasing EEMT. Decreased denudation rate at high EEMT is likely related to increasing regolith depth. Rates of soil production decrease with increasing regolith depth (e.g., Heimsath et al. 1997) because regolith cover acts as a buffer for the underlying bedrock, protecting it from the diurnal temperature changes and infiltrating runoff that drive subsurface weathering (Minasny and McBratney 1999). As noted below, regolith depth increases linearly with EEMT above F_{BIO} of 0.5 suggesting the negative functions noted in the denudation data are indirectly controlled by regolith depth. Regardless of the mechanism, the data suggest strong coupling of exergy flux to denudation at high EEMT, whereas factors other than EEMT, such as variation in rock chemistry or uplift rates, exert greater control over denudation in low EEMT systems where most exergy is partitioned to carbon production and cycling.

Short-term watershed-based and long-term regolith-based chemical denudation rates demonstrate inverse patterns for high EEMT sites (Figs. 3, 4c). The reasons are unclear, but may result from the disparate time scales of the respective methods, i.e., watershed efflux integrating over annual time scales and regolith denudation integrating millennial time scales. For example, over geologic time scales,

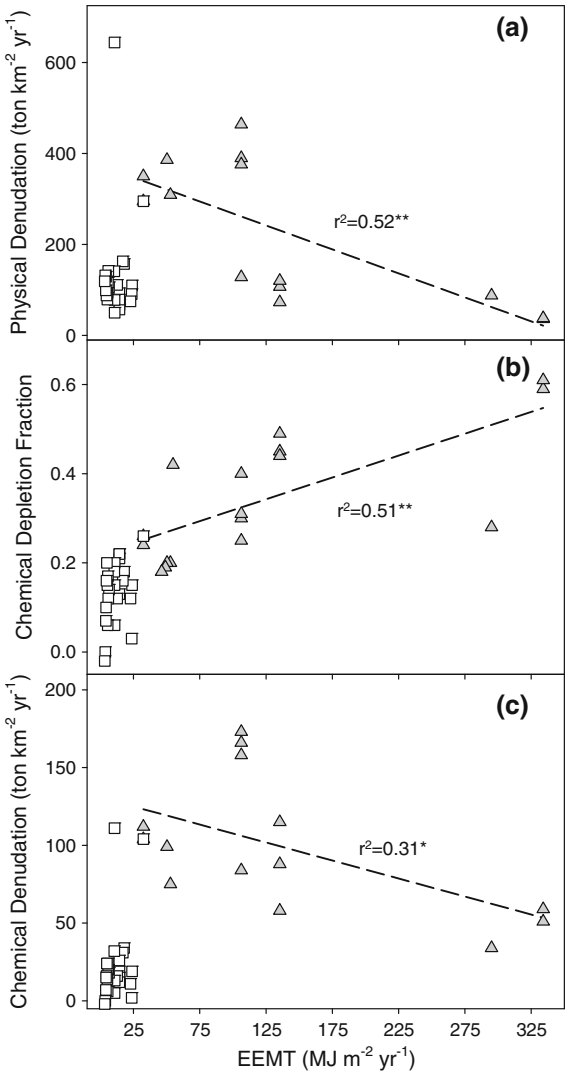

Fig. 4 Physical denudation rate **a** the chemical depletion fraction **b** and chemical denudation rate **c** relative to effective energy and mass transfer (EEMT). Open squares are sites where $F_{BIO} > 0.5$ and gray triangles sites of $F_{BIO} < 0.5$ where F_{BIO} is the fraction of EEMT derived from net primary production. Dashed lines represent linear regression models fit between each variable and EEMT for $F_{BIO} < 0.5$ sites. Denudataion data taken from Riebe et al. (2004) and EEMT calculated from mean annual temperature and precipitation following Rasmussen and Tabor (2007)

steady-state regolith depth implies physical denudation controls the rate of "fresh" mineral supply and hence the potential rate of chemical denudation (West et al. 2005). High EEMT sites exhibit low physical denudation rates and deep regolith profiles (see below) suggesting reduced rates of mineral supply and chemical weathering focused on a fixed, but large volume of minerals. Integrated over geologic times scales this manifests as reduced rates of chemical denudation because of the low rate of mineral turnover. However, high annual rates of flow exergy dominated by water flux through the subsurface reacting with a large volume of partially weathered minerals may result in relatively high short-term chemical depletion rates and solute efflux to surface waters.

Effective energy and mass transfer and regolith depth

The depth to the regolith weathering front in granitic terrain (Rasmussen et al. 2009) exhibits relations to EEMT similar to the denudation rates noted above, i.e., significant linear relationship with increasing EEMT in sites with $F_{BIO} < 0.5$ (Fig. 5). Detailed data analysis indicates that the depth to weathering front is a nonlinear function of EEMT for sites where $F_{BIO} > 0.5$ (Fig. 5 inset), similar in form and shape to functions derived by Rasmussen and Tabor (2007) and expanded upon by Pelletier and Rasmussen (2009) relating EEMT to regolith depth. These data further highlight the substantial variation in critical zone structure according to both EEMT and the relative partitioning of EEMT to carbon and water fluxes and a significant nonlinear transition in critical zone structure.

Building upon the noted relationship between regolith depth and EEMT, Pelletier and Rasmussen (2009) demonstrated that EEMT may be used to model the interactive control of radiant, geochemical and elevational gradients on regolith depth, erosion rate, and soil residence time. The model was based on a coupling of EEMT with traditional geomorphic transport laws defining regolith depth relative to the maximum bedrock lowering rate and uplift: $H_S = H_0 \ln (P_0/U)$, where H_S is regolith depth, H_0 a reference depth, P_0 is maximum bedrock lowering rate, equivalent to maximum soil production rate, and U is uplift rate. A nonlinear function between EEMT and P_0 based on empirical field data was used to estimate bedrock lowering rates: $P_0 = ae^{b \cdot \mathrm{EEMT}}$, where a and b are fitting parameters that vary with lithology and thereby capture geochemical variation in lithology. The modeled results indicate a threshold type interaction between EEMT and uplift rate whereby once a certain EEMT threshold is exceeded, the rate of soil production exceeds uplift with

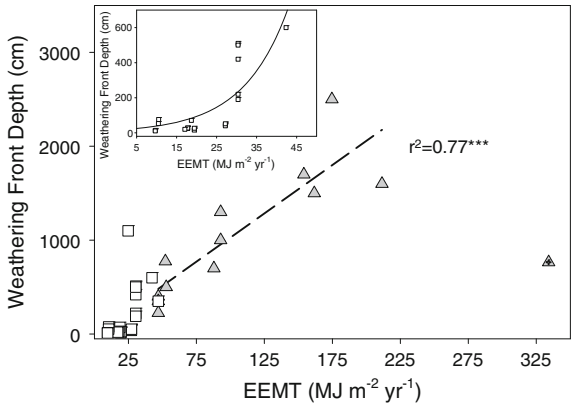

Fig. 5 Depth to weathering front as determined by sodium depletion profiles relative to effective energy and mass transfer (EEMT). The open squares are sites of $F_{BIO} > 0.5$ whereas gray triangles are sites of $F_{BIO} < 0.5$ where F_{BIO} is the fraction of EEMT derived from net primary production. The dashed line is the regression line between EEMT and weathering front depth for sites with $F_{BIO} < 0.5$. The site noted with gray triangle and cross-hair was not included in the linear regression as it was determined to be statistical outlier according to a Mahalanobis distance analysis. Depth data from Rasmussen et al. (2009) and EEMT calculated from mean annual temperature and precipitation following Rasmussen and Tabor (2007)

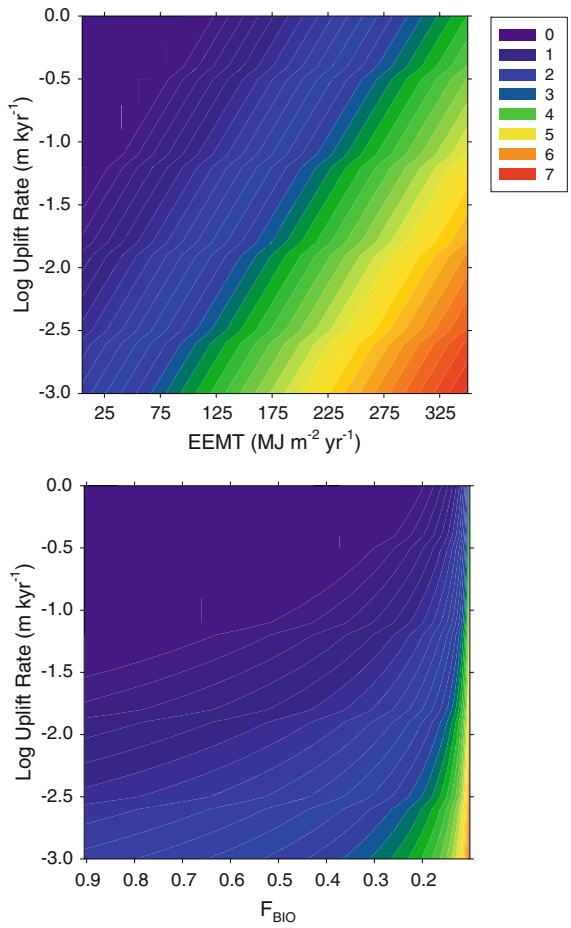

Fig. 6 Modeled relationship of regolith depth (m) to relative to effective energy and mass transfer (EEMT) and uplift rate (**a**) and regolith depth relative to F_{BIO} and uplift rate (**b**) where F_{BIO} is the fraction of EEMT derived from net primary production. The legend indicates modeled regolith depth grading from zero or bare rock in purple to greater than 7 meters in red. Data taken from Pelletier and Rasmussen (2009)

resultant increase in regolith depth (Fig. 6a). In addition, these data indicate a highly nonlinear relation between uplift, F_{BIO} and regolith depth in that $F_{BIO} = 0.5$ notes the transition from a near linear to nonlinear increase of regolith depth with decreasing F_{BIO} regardless of uplift rate (Fig. 6b).

The interactive control of radiant and elevation gradients on erosion and regolith development has been demonstrated in other recent modeling exercises (Phillips 2009; Yoo et al. 2005). Both of these studies indicate that only a fraction, i.e., <1%, of the exergy flux from primary production is sufficient to exert substantial control over the redistribution of sediment on the landscape. In addition, both of these studies quantified the gradient interactions in units of J m^{-2} s^{-1}, presenting excellent additional examples for the potential of coupling interdisciplinary research, in this case ecology and geomorphology, through exergy flux terms.

Effective energy and mass transfer and soil development

Global soil (Soil Survey Staff 2005) and climate (New et al. 1999) datasets indicate substantial variation in EEMT by soil taxonomic class (Fig. 7). The variance in median values for EEMT by soil taxa correspond to geographic and climatic limits to soil distribution, and to the relative degree of weathering associated with specific soil taxa. For example, Gelisols are limited to areas with permafrost at high latitudes and correspondingly exhibit very low EEMT following the global EEMT patterns noted above (Fig. 2a). The tightly constrained EEMT distribution in Aridisols, Mollisols and Spodosols also corresponds with the constraint of these soils to specific climatic regimes. In contrast, Entisols and Inceptisols exhibit large variance relative to Aridisols, Mollisols or Spodosols. Entisols and Inceptisols develop in a wide range of soil forming environments where their weakly weathered

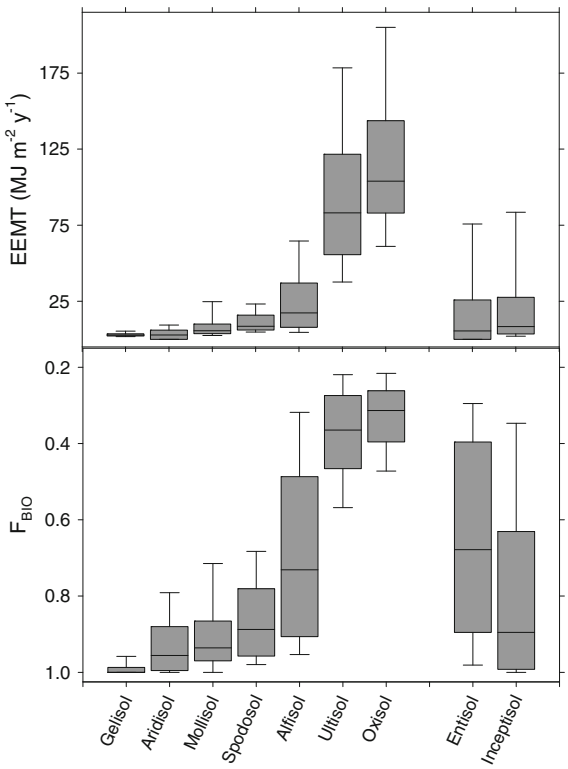

Fig. 7 Box plots demonstrating the relative distribution of effective energy and mass transfer (EEMT) and the fraction of EEMT from net primary production (F_{BIO}) by Soil Order, excluding Histosols, Vertisols, and Andisols. Entisols and Inceptisols are plotted separately because of the wide range of environments in which these soils occur

state may be less a function of exergy flux, but more related to other factors such as landscape age, elevation gradients, or parent material and geochemical gradients. There is also an apparent EEMT threshold grading from Alfisols to Ultisols and Oxisols from 25 to 75 MJ m^{-2} yr^{-1} corresponding to the transition to E_{PPT} dominance (Fig. 7). This break corresponds to the transition to highly weathered and chemically depleted soils and matches the patterns noted above for denudation and regolith depth. In addition, the noted EEMT relationships by soil taxa correspond well with the theoretical pedogenic energy scheme presented by Smeck et al. (1983) and previous landscape and regional scale EEMT analyses (Rasmussen et al. 2005; Rasmussen and Tabor 2007). These data, and those presented above, all indicate substantial variation in critical zone structure and development as a function of EEMT and the relative partitioning of EEMT to carbon water.

Concluding remarks

The data synthesis presented herein demonstrates a significant *empirical* linkage between effective energy and mass transfer with measurable critical zone structural and functional properties. Consistent with open system thermodynamics, the energy and mass transfer model predicts that structural organization and process-level heterogeneity within the critical zone increases with increasing energy input. In particular, a central theme among the independent datasets and model results is that substantial variation in critical zone structure and function occurs with (i) increasing flow exergy, and (ii) at the transition between systems dominated by carbon flux to those dominated by water flux.

The model as currently derived is fundamentally empirical, but is based on simple energy and mass balance and grounded in open system, non-equilibrium thermodynamics. Its strength lies in its simplicity, its low requirements for fitted parameterization (EEMT can be calculated from meteorological data alone), and its apparent predictive power. The EEMT parameter provides a means for translating climatic inputs (temperature and precipitation) into an "energy currency", thereby quantifying the capacity of climate, as modulated by primary production and effective precipitation, to do work on the critical zone. The framework is inherently interdisciplinary in that production of EEMT is ultimately driven by solar radiation and related climatic forces that interact with and act as feedbacks to biologic production, biogeochemical cycling, and landscape evolution. One key advantage to the energy-based framework is the common units for linking multiple earth surface processes across time and space. In addition to the synthesis here, the recent studies of Phillips (2009) and Yoo et al. (2005) noted above also provide excellent examples of how energy units may be effectively used to couple geomorphic processes. Energy and thermodynamic potential is also a common currency among ecological (e.g., DeWulf et al. 2008) and geochemical models (e.g., Lasaga et al. 1994), further indicating the potential for developing quantitative linkages among these disciplines using a common energy term such as EEMT.

We present a theoretical framework for quantifying controls of critical zone function and development. The energy-based framework provides a means to quantitatively constrain critical zone evolution and

predict rates of critical zone processes. The thermodynamic formulation may be directly tested in well constrained natural and artificial systems with varying geochemical, radiant and gravitation forcing and relative rates of effective energy and mass transfer. The framework will aide in predicting and constraining critical zone evolution by providing a means to identify nonlinearities and landscape divergence from a predicted thermodynamic equilibrium and/or steady-state related to both the magnitude of energy and mass transfer and the partitioning of flow exergy to primary production and subsurface water flux.

Acknowledgements We acknowledge the University of Arizona Critical Zone Work Group that contributed to discussion and framework development, including Dave Breshears, James Hogan, Shirley Kurc, Kathleen Lohse, Jennifer McIntosh, Tom Meixner and Marcel Schaap. This work was supported by B2 Earthscience through the Philecology Foundation, and National Science Foundation grants DEB-0418134, DEB-0415977, DEB-0543130, EAR-0632516, EAR-0724958, and the National Science Foundation Science and Technology Center for Sustainability of semi-Arid Hydrology and Riparian Areas (SAHRA).

References

Anderson DW (1995) Decomposition of organic matter and carbon emissions from soils. In: Lal R, Kimble J, Stewart BA (eds) Soils and global change. Lewis Publishers, Boca Raton, FL, pp 165–175

Brantley SL, White TS, White AF, Sparks D, Richter D, Pregitzer K, Derry L, Chorover J, April R, Anderson S, Amundson R (2006) Frontiers in exploration of the critical zone: Report of a workshop sponsored by the National Science Foundation. p 30

Arkley RJ (1963) Calculation of carbonate and water movement in soil from climate data. Soil Sci 96:239–248

Balzhiser RE, Samuels MR, Eliassen J (1977) Engineering thermodynamics. Prentice-Hall, Englewood Cliffs, NJ

Bastianoni S, Pulselli FM, Rustici M (2006) Exergy versus emergy flow in ecosystems: is there an order in maximizations? Ecol Indic 6:58–62

Bejan A (2006) Advanced engineering thermodynamics. Wiley, Hoboken, NJ

Bendoricchio G, Jorgensen SE (1997) Exergy as goal function of ecosystems dynamic. Ecol Modell 102:5–15

Blum WEH (2008) Forms of energy involved in soil and sediment processes. J Soils Sediments 8:1–2

Botkin DB, Malone CR (1968) Efficiency of net primary production based on light intercepted during growing season. Ecology 49:438–444

Buol SW, Southard RJ, Graham RC, McDaniel PA (2003) Soil genesis and classification, 5th edn. Iowa State Press, Ames, IA

Chorover J, Kretzschmar R, Garcia-Pichel F, Sparks DL (2007) Soil biogeochemical processes within the critical zone. Elements 3:321–326

Dewulf J, Van Langenhove H, Muys B, Bruers S, Bakshi BR, Grubb GF, Paulus DM, Sciubba E (2008) Exergy: its potential and limitations in environmental science and technology. Environ Sci Technol 42:2221–2232

Dietrich W, Bellugi DG, Sklar L, Stock JD, Heimsath AM, Roering JJ (2003) Geomorphic transport laws for predicting landscape form and dynamics. In: Wilcock PR, Iverson RM (eds) Prediction in geomorphology. American Geophysical Union, Washington, DC, pp 103–132

Dokuchaev VV (1967) Selected works of V.V. Dokuchaev. Israel program for scientific translations. Available from the U.S. Dept. of Commerce, Clearinghouse for Federal Scientific and Technical Information, Jerusalem; Springfield, VA

Evett SR (2000) Energy and water balances at soil-plant-atmosphere interfaces. In: Malcom ES (ed) Handbook of soil science. CRC Press, Boca Raton, pp A-129–A178

Farrar JF (1985) The respiratory source of CO_2. Plant Cell Environ 8:427–438

Heimsath AM, Dietrich WE, Nishiizumi K, Finkel RC (1997) The soil production function and landscape equilibrium. Nature 388:358–361

Hutchinson GE (1957) Concluding remarks. Cold Spring Harb Symp Quantitative Biol 22:415–427. (Reprinted in 1991: Classics in theoretical biology. Bull Math Biol 53:193–213)

Jenny H (1941) Factors of soil formation; a system of quantitative pedology. McGraw-Hill Book Company, Inc., New York, London

Jenny H (1961) Derivation of state factor equations of soils and ecosystems. Soil Sci Soc Am J 25:385–388

Jorgensen SE, Fath BD (2006) Examination of ecological networks. Ecol Modell 196:283–288

Jørgensen SE, Fath BD (2004) Application of thermodynamic principles in ecology. Ecol Complex 1:267–280

Kay JJ (2000) Ecosystems as self-organizing holarchic open systems: narratives and the second law of thermodynamics. In: Jørgensen SE, Müller F (eds) Handbook of ecosystem theories and management. Lewis Publishers, Boca Raton, FL, pp 135–160

Kleidon A (2009) Nonequilibrium thermodynamics and maximum entropy production in the earth system. Naturwissenschaften 96:653–677

Kleidon A, Lorenz RD (2005) Entropy production by earth system processes. In: Kleidon A, Lorenz RD (eds) Nonequilibrium thermodynamics and the production of entropy/life, earth, and beyond. Springer, Berlin, pp 1–16

L'vovich MI (1979) World water resources and their future. Original in Russian. English translation American Geophysical Union, Washington, DC

Lasaga AC, Soler JM, Ganor J, Burch TE, Nagy KL (1994) Chemical-weathering rate laws and global geochemical cycles. Geochim Cosmochim Acta 58:2361–2386

Lieth H (1975) Primary production of the major vegetation units of the world. In: Leith H, Whittaker RH (eds) Primary productivity of the biosphere. Springer-Verlag, NY, pp 203–215

Lindeman RL (1942) The trophic-dynamic aspect of ecology. Ecology 23:399–418
Lotka AJ (1922) Contribution to the energetics of evolution. Proc Natl Acad Sci USA 8:147–151
Lovett G, Cole J, Pace M (2006) Is net ecosystem production equal to ecosystem carbon accumulation? Ecosystems 9:152–155
Minasny B, McBratney AB (1999) A rudimentary mechanistic model for soil production and landscape development. Geoderma 90:3–21
Morowitz HJ (1968) Energy flow in biology; biological organization as a problem in thermal physics. Academic Press, New York
New M, Hulme M, Jones PD (1999) Representing twentieth century space-time climate variability. Part 1: development of a 1961–1990 mean monthly terrestrial climatology. J Clim 12:829–856
Nicolis G, Prigogine I (1989) Exploring complexity. W. H. Freeman, New York
NRC (2001) Basic research opportunities in earth sciences. National Academies Press. National Research Council, Washington, DC
NRC (2009) Landscapes on the edge: new horizons for research on earth's surface. The National Acadamies Press, Washington DC
Odum HT (1988) Self-organization, transformity, and information. Science 242:1132–1139
Odum HT, Pinkerton RC (1955) Times speed regulator—the optimum efficiency for maximum power output in physical and biological systems. Am Sci 43:331–343
Osmond CB, Winter K, Ziegler H (1982) Functional significance of different pathways of CO_2 fixation in photosynthesis. In: Person A, Zimmerman MH (eds) Encyclopedia of plant physiology. Springer, New York, pp 479–547
Pelletier JD (2008) Quantitative modeling of earth surface processes. Cambridge University Press, New York
Pelletier JD, Rasmussen C (2009) Quantifying the climatic and tectonic controls on hillslope steepness and erosion rate. Lithosphere 1:73–80
Phillips JD (2009) Biological energy in landscape evolution. Am J Sci 309:271–289
Rasmussen C, Tabor NJ (2007) Applying a quantitative pedogenic energy model across a range of environmental gradients. Soil Sci Soc Am J 71:1719–1729
Rasmussen C, Southard RJ, Horwath WR (2005) Modeling energy inputs to predict pedogenic environments using regional environmental databases. Soil Sci Soc Am J 69:1266–1274
Rasmussen C, Williams JZ, Brantley S, Richter D, White A, April R (2009) Climatic controls of regolith weathering and mass flux in granitic terrain—a synthesis of Critical Zone Exploration Network data. Geochimica Et Cosmochimica Acta 73:A1074–A1074
Reiners WA (1972) Structure and energetics of 3 Minnesota forests. Ecol Monogr 42:71–94
Reheis MC (2006) A 16-year record of dust deposition in southern Nevada and California, USA. J Arid Environ 67:487–520
Riebe CS, Kirchner JW, Granger DE, Finkel RC (2001) Strong tectonic and weak climatic control of long-term chemical weathering rates. Geology 29:511–514
Riebe CS, Kirchner JW, Finkel RC (2004) Erosional and climatic effects on long-term chemical weathering rates in granitic landscapes spanning diverse climate regimes. Earth Planet Sci Lett 224:547–562
Rinaldo A, Rodriguez-Iturbe I, Rigon R (1998) Channel networks. Annu Rev Earth Planet Sci 26:289–327
Runge ECA (1973) Soil development sequences and energy models. Soil Sci 115:183–193
Schlesinger WH (1997) Biogeochemistry: an analysis of global change. Academic Press, San Diego, CA; London
Sivapalan M (2005) Pattern, process and function: elements of a unified theory of hydrology at the catchment scale. In: Anderson M (ed) Encyclopedia of hydrological sciences. Wiley, New York
Smeck NE, Runge ECA, Mackintosh EE (1983) Dynamics and genetic modeling of soil systems. In: Wilding LP, Smeck NE, Hall GF (eds) Pedogenesis and soil taxonomy. Elsevier, New York, pp 51–81
Smil V (1991) General energetics: energy in the biosphere and civilization. Wiley Interscience, New York
Soil Survey Staff (2005) FAO-UNESCO soil map of the world; http://soils.usda.gov/use/worldsoils/mapindex/order.html. USDA-NRCS Soil Survey Division, World Soil Resources, Washington, DC
Volobuyev VR (1964) Ecology of soils. Academy of Sciences of the Azerbaidzn SSR. Institute of Soil Science and Agrochemistry, Israel Program for Scientific Translations, Jersualem
Volobuyev VR (1974) Main concepts of soil ecology. Geoderma 12:27–33
Volobuyev VR (1983) Thermodynamic basis of soil classification. Soviet Soil Sci 15:71–83
Wagendorp T, Gulinck H, Coppin P, Muys B (2006) Land use impact evaluation in life cycle assessment based on ecosystem thermodynamics. Energy 31:112–125
West AJ, Galy A, Bickle M (2005) Tectonic and climatic controls on silicate weathering. Earth Planet Sci Lett 235:211–228
White AF, Blum AE (1995) Effects of climate on chemical-weathering in watersheds. Geochim Cosmochim Acta 59:1729–1747
White AF, Brantley SL (2003) The effect of time on the weathering of silicate minerals: why do weathering rates differ in the laboratory and field? Chem Geol 202:479–506
White AF, Blum AE, Bullen TD, Vivit DV, Schulz M, Fitzpatrick J (1999) The effect of temperature on experimental and natural chemical weathering rates of granitoid rocks. Geochim Cosmochim Acta 63:3277–3291
Woods TL, Garrels RM (1987) Thermodynamic values at low temperature for natural inorganic materials: an uncritical summary. Oxford University Press, NY, 242 pp
Yoo K, Amundson R, Heimsath AM, Dietrich WE (2005) Process-based model linking pocket gopher (Thomomys bottae) activity to sediment transport and soil thickness. Geology 33:917–920